Penerbit Akademia Baru

Malaysian Journal on Composites Science and Manufacturing

Journal homepage:
https://www.akademiabaru.com/submit/index.php/mjcsm/
ISSN: 2716-6945

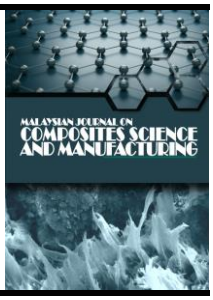

Performance Analysis of a Designed Prototype of a Motor Coupled Variable Inertia Flywheel System

Open Access

Syed Munimus Salam[1,*], Muhammad Mahbubur Rashid[1]

[1] Department of Mechatronics Engineering, International Islamic University Malaysia, Selangor, Malaysia

ARTICLE INFO

Article history:
Received 2 September 2023
Received in revised form 22 September 2023
Accepted 30 October 2023
Available online 30 November 2023

Keywords:
VIF, Power, Induction Motor, Energy Saving

ABSTRACT

The presence of a substantial moment of inertia in a flywheel poses challenges at the initiation of rotation in a rotating machine. During stable operation at high velocities, several energy-saving advantages can be efficiently attained, allowing for the potential of achieving adequate energy savings in specific applications. One potential solution to address this issue is the implementation of a flywheel that possesses the ability to modify its moment of inertia. While it is possible to derive the concept of variable inertia by adjusting the radii of the masses in relation to the axis of the flywheel, the techniques employed to regulate the variable inertial flywheel are rather intricate. This study presents an implementation of a variable inertia flywheel system coupling with electrical machinery to reduce power consumption. The main objective of the study is to reduce energy consumption utilizing variable inertia flywheel. Under various motion scenarios, the advanced machine's dynamic reaction is examined. Finally, a standard testing method demonstrates almost ninety seven percent similarity between an analytical and practical analysis.

1. Introduction

Though a wide range of systems are available for energy conservation, the flywheel is one of the easiest to consider for the conservation of angular momentum to store rotational energy. Flywheels are now the best option for many applications because they have great qualities such as a long lifespan, high power density, low capital costs for short-term storing energy (from seconds to a few minutes), and lengthy cyclic endurance [1,2]. Flywheels have been used in various applications, mainly to store energy or reduce shaft angular velocity variability. Flywheel hybrid cars, intermittent power supplies, wind turbines, and space power systems are a few examples of applications for energy storage. Flywheels are used in various industrial applications, including AC generators,

* *Corresponding author.*
E-mail address: s.munimus@live.iium.edu.my (Syed Munimus Salam)
E-mail of co-author: mahbub@iium.edu.my

https://doi.org/10.37934/mjcsm.12.1.6272

camshafts, and internal combustion engines, to smooth out angular velocity irregularities [3]. A variable-inertia flywheel's design must be more sophisticated than a constant-inertia flywheel's. A flywheel needs to have flexible geometry around its spin axis to have a controlled moment of inertia about that axis and change the geometry for the moving parts inside it [4].

Even though a variable inertia flywheel (VIF) might be more complicated and, therefore, heavier per unit of energy stored than a fixed inertia flywheel, if it is thought that the VIF is replacing both the flywheel and the gearbox, it might still have a higher energy density than the constant inertia flywheel. The design and implementation of VIF in power savings and stability received primary focus in most research [7–15], without considering the impact of high system stability. The variable inertia control may be unstable under conditions of load disruptions, which can cause instability and system failure. The main flaw with the strategies is the described problem. All previous virtual inertia designs and methodologies could not provide stable control without considering the consequences of the applied device. Therefore, to handle changes in a machine with significant stability and energy savings, a strong adaptive control approach must be implemented in addition to inertia control.

This flywheel's energy-saving capabilities have received extensive attention during the past few decades. Alhrshy *et al.* [6] have proposed integrating a flywheel energy storage system into a wind turbine rotor. According to Figliotti and Gomes [7], they designed a spring-connected variable-inertia flywheel directly tied to the vehicle. The fluidic variable-inertia flywheel proposed by Van de Ven [8], can maintain its angular velocity over a wide range of energy storage. Ishida *et al.*[9] found that a centrifugal pendulum has been incorporated into the double-mass flywheel. The fluidic variable-inertia flywheel suggested by Braid [10] can maintain a constant angular velocity over a wide range of energy storage. The standard fixed-inertia flywheel can be replaced by a variable-inertia flywheel, according to Yuan *et al.* [11]. Flywheels with a changeable equivalent mass moment of inertia and without a fixed connection to the machine's input shaft were introduced by Bao *et al.* [12]. New vibration suppression devices were proposed by Matsuoka [13] by using a fluid that operated like a series of inertia masses. On the other hand, magnetorheological fluid has not been widely used in flywheels. VIMRF (variable inertia magnetic rheological flywheel) is yet to be studied for its energy-saving potential compared to its rivals. Alternate methods are developing with respect to research progress. Though there are many literatures available [8-13] on variable inertia flywheel, a poor amount addressed on the application side energy saving capability. The main gap in the previous literature is only designing the VIF but less concentration on its application. This paper focuses on the application of a designed prototype of VIF coupled with induction motor and finding the energy saving benefit of the system both by simulation and prototyping.

2. Problem Statement

First, the design of a variable-inertia flywheel will be more complicated than that of a constant-inertia flywheel. To have an adjustable moment of inertia for a flywheel about its spin axis, the geometry around that axis needs to be flexible, and the flywheel needs to have moveable components to change the geometry [14]. Although the concept of variable inertia may be utilized by varying the distances of the masses from the flywheel's axis, the VIF's controlling mechanisms are somewhat complicated. Also, a lot of information is available regarding VIF control approaches, but little of it focuses on their application side. The primary goal of this research is to reduce the energy consumption of the applied rotating electric machine and thus obtain a more efficient output from the VIF-coupled rotating machines. A simulated system has also been created to characterize system parameters.

3. Methodology

Once the necessary information has been gathered to build a Variable Inertia Flywheel (VIF), a simulation is implemented to determine the performance curve. The subsequent step in the investigation was developing a simulated model, which was then used to design and construct a prototype of a VIF in conjunction with a three-phase induction motor. Performance data was collected at the Mechatronics Electrical Lab at the International Islamic University Malaysia (IIUM), followed by a subsequent comparison with simulated data. As seen in Figure 1, the design was precisely derived from the initial profile of the simulated system.

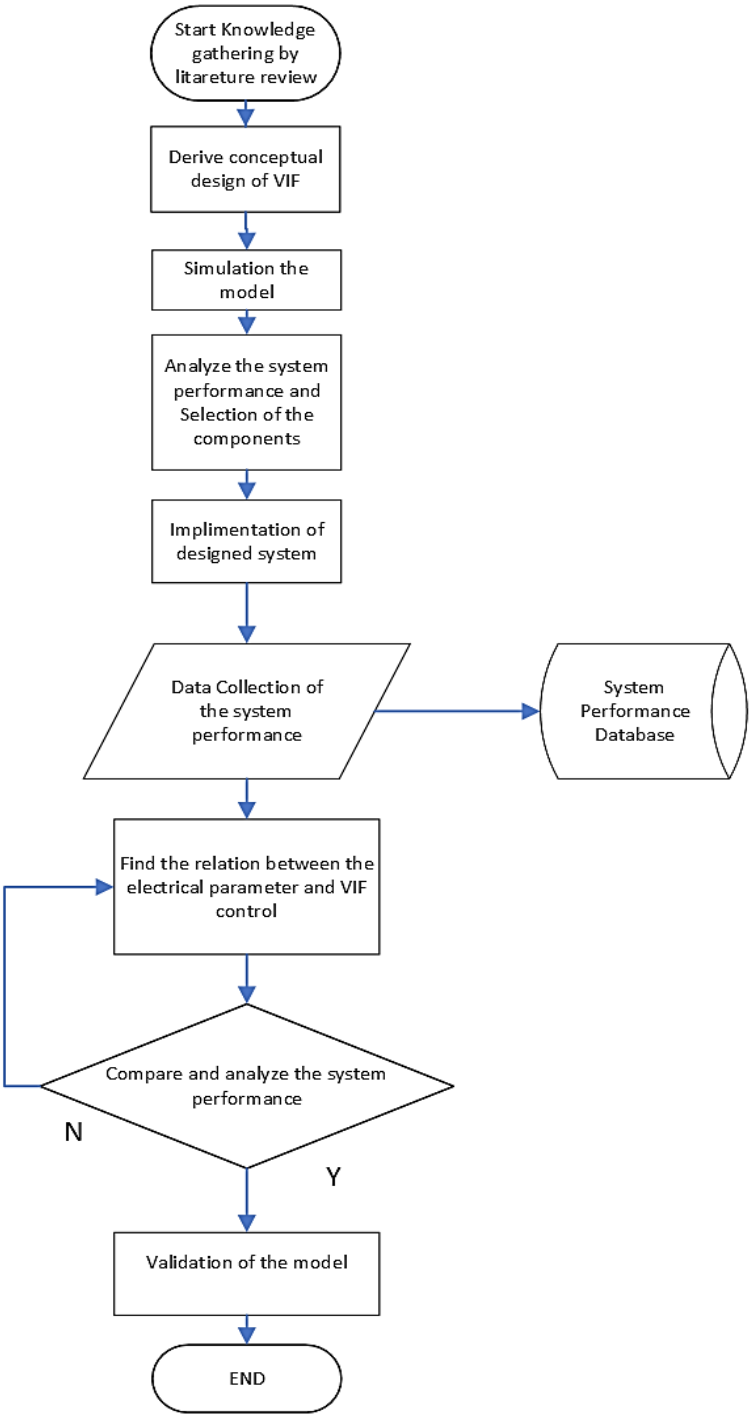

Fig. 1. Flowchart of the methodology of the research process

When choosing the right inertia for VIF settings to keep the motor speed steady while using the least amount of electricity, the control model is optimized by considering the flywheel system and other motor system features that are related to it. All relevant research was initially analyzed, and the VIF system's mathematical equations were studied. For bidirectional energy transmission to the flywheel, an induction machine is suggested after system modelling for simulation. A mechanical interface connects the flywheel to the induction motor if the motor load changes. This coupling interface is employed for charging and discharging the flywheel as a mechanical battery. The control system is utilized to enhance the inertia of the induction machine before it reaches a sufficient speed, and then an external control system identifies the need for inertia and adjusts the speed at the point of common coupling with the machine using an optimal control system to maintain inertia.

3.1 Design Structure

A flywheel with a lower moment of inertia is required for a vehicle operating at low torque. Still, historically, a flywheel with a constant inertia and a higher mass moment of inertia has been employed to smooth out torque variations at high speeds and torque. As a result, the engine is compelled to provide the shaft with its maximum power while operating at low torque. A flywheel with constant inertia cannot power a mechanical system operating at a wide range of changing speeds. The researchers tried a variable inertial flywheel as a possible alternative. Still, they could not achieve a smooth fluctuation of inertia due to their lack of expertise in stabilizing the flywheel at required radii at various speeds/torques.

3.2 Mathematical Representations

The moments of inertia for the actuator and the immovable structural component, each about their own mass centres as well as the shaft centre, are written as the following:

$$J_s = \frac{1}{4} M_s \left(\frac{d_s^2}{4} + \frac{I_s^2}{3}\right) \tag{1}$$

$$J_F = J_{shaft} + J_{scd} - N J_{slot} \tag{2}$$

where,

$J_{scd} = \frac{1}{4} M_{scd}(r_s^2 + r_0^2)$ is the polar moment of inertia of a solid flywheel of uniform thickness

J_{shaft} is the polar moment of inertia of the shaft [15]

$$J_{slot} = m_{slot}\left\{\frac{1}{12}(d_s^2 + I_{slot}^2) + (r_0 + 0.5 I_{slot})^2\right\} \tag{3}$$

A pre-compressed spring is set between the piston and the frame. The coil is entangled in the double-ring groove of the piston. If we consider friction force, F_f , the spring force, F_0, MR damping force F_{mrf}, sin w is a sign function related to the radial slip velocity of the piston, and k is the spring constant [16],

$$J_{slot} = m_{slot}\{F_0 + (F_{mrf} + F_f) Sin\, w + k \frac{r_i}{m_{slot} w^2 - k} \tag{4}$$

3.3 System Simulations

The electric motor, losses, and valve details are considered while creating the model, along with the flywheels' manufacturing characteristics. The following few presumptions are made:

- The dynamics of the springs are not considered in the model, and their properties are assumed to be linear.
- The effect of gravity on the slider is not considered.
- When the spring is at its shortest length, it is not distorted.

Considering all these phenomena, a simulation diagram has been developed in the Matlab-Simulink platform, as shown in Figure 2.

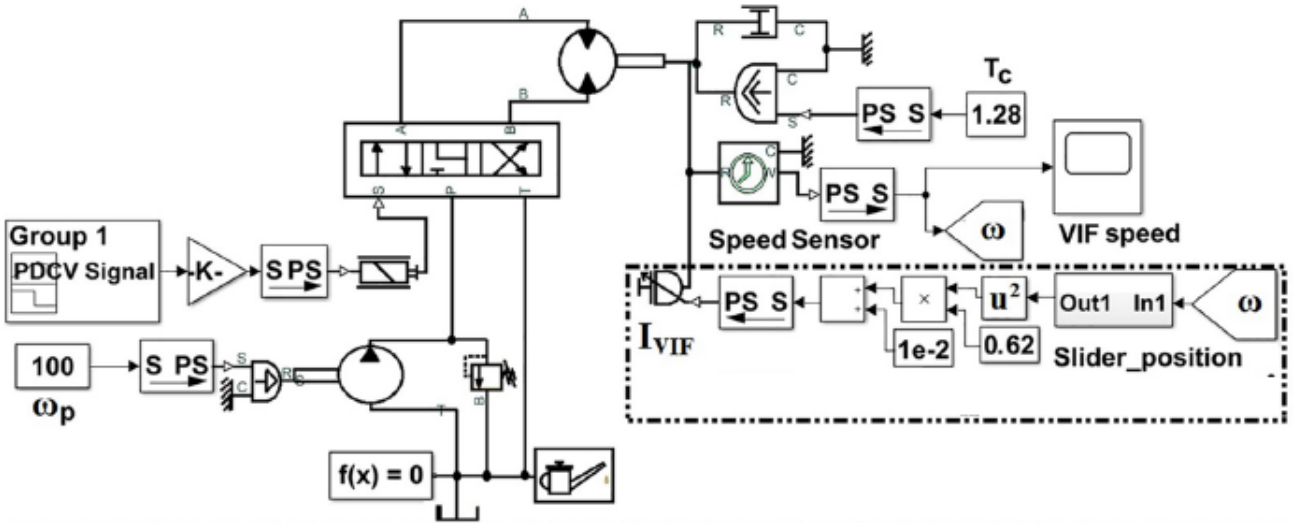

Fig. 2. VIF Simulation diagram in Matlab-Simulink platform

As the Figure 2 illustrates, motor current usage varies in relation to a constant voltage. Furthermore, the speed-building criteria are displayed, and it is discovered that without VIF, the total speed quickly stabilized. Consumption has changed due to the torque's temporal volatility. Each wind consumes nearly the same amount of current during the entire cycle.

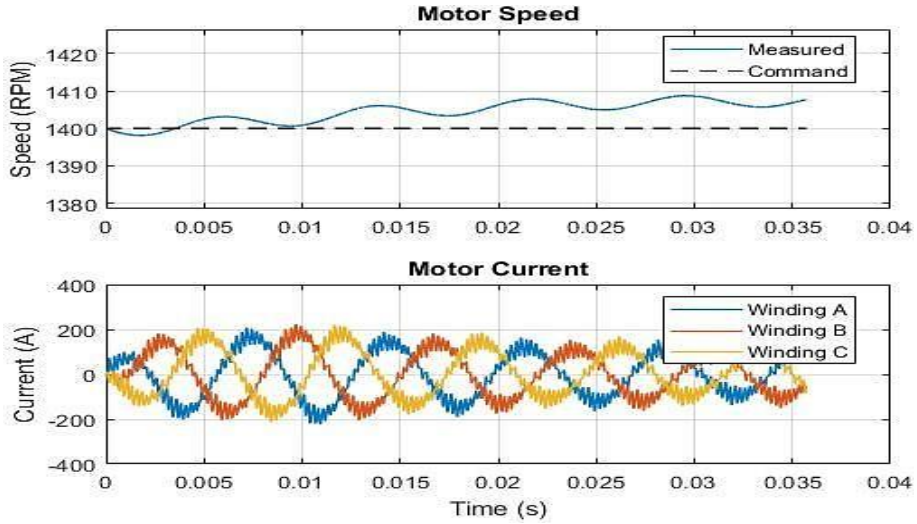

Fig. 3. A diagram of a motor current with VIF

The VIF part depicts the characteristics of speed build-up using a VIF-integrated system. Even if there is a depiction of an unstable method, the speed steadily increases with respect to time due to the VIF mechanism. It will eventually become stable with respect to time. Finally, decreased power consumption is caused by lowering winding current consumption (Figure 3). As a result, the power consumption may be reduced while the VIF can store the same amount of energy.

Figure 3 shows the output current consumption value of a three-phase induction motor. The number gradually declines until reaching a state of stability at 160 Amperes. Conversely, the velocity is seeing an upward trend in relation to minimal energy use.

3.4 System Implementations

Subsequently, the next step of action entailed the execution of the variable-inertia flywheel prototype. The flywheel components are depicted in Figure 4. The primary structure, denoted as 1, consists of a stationary inertia flywheel housing four internal ducts designed to accommodate varying masses. Cylinder-shaped components labelled with the number 5 are put into these conduits. Each cylindrical component is characterized by a variable mass denoted as 4 and contains spring elements denoted as 2 inside its structure. When the flywheel is set in motion, the upward movement of inertia occurs due to the rotational speed's moment of inertia. The details of the flywheel are described in Table 1.

Fig. 4. Components of Variable Inertia Flywheel

Table 1
The parts of VIF with the parameter value

Name of component model	Quantity
Damper mass	2 Kg
Damper diameter	20 mm
Designed energy storage	300 wh
Designed energy storage	300 wh
Maximum speed	1400 rmp
Flywheel radius	60 mm
Mass of single piston	250 gm
Flywheel weight	10.5 kg
Current rating	5 amp

The generated current, total electrical power usage, frequency, and power factor are monitored using a multimeter and oscilloscope. Table 2 presents comprehensive performance statistics. Furthermore, a graphical data analysis has been incorporated in the last portion.

4. Results and Data Comparison

This equipment combination, in conjunction with VIF, is employed in a motor application to evaluate the energy savings of various speed conditions and placements within the system. The primary objective of this study is to determine the energy-saving potential of a flywheel system for a given device and to compare the results obtained from both simulated and real-world scenarios. Furthermore, the evaluation of speed growth is conducted by analyzing motor performance.

4.1 Short Period Starting Parameter Considerations

Table 2
The induction motor power calculating parameter values for with and without VIF

Time	With VIF	Without VIF
Second	Volt, Amp, PF	Volt, Amp, PF
1st	239.8, 5.9, 0.39	239.9, 5.1, 0.41
2nd	230.8, 6.3, 0.38	232.9, 5.3, 0.40
3rd	232.9, 5.3, 0.40	239.9, 4.8, 0.47
4th	238.8, 4.3, 0.50	239.9, 4.7, 0.47
5th	238.7, 4.1, 0.50	239.9, 4.6, 0.48
6th	238.7, 4 , 0.50	239.9, 4.6, 0.49
7th	238.6, 4 , 0.50	239.8, 4.5, 0.49
8th	238.7, 3.9, 0.50	239.8, 4.5, 0.49
9th	238.7, 4 , 0.50	239.9, 4.6, 0.50
10th	238.7, 4 , 0.50	239.9, 4.6, 0.50

Initially, a comparison is made between the initial simulation features and prototype performance. Table 2 comprehensively compares the VIF system and the fixed flywheel method. In the context of VIF, power consumption exhibits a gradual decline, but in fixed systems, it remains constant. Moreover, due to the variable mass in the adjusted system, the inertia with respect to time will be modified, resulting in a decrease in current consumption for each winding in the case of VIF.

The graphical analysis depicted in Figure 5 reveals a discernible temporal variation in the overall consumption. In variable-speed dynamic systems, using a flywheel with a substantial moment of inertia is crucial as it mitigates the adverse effects of large angular velocity variations. The data shown in Figure 5 indicates that the power consumption during the first phase is the largest due to the relatively lower moment of inertia. Once the ideal threshold is attained, the value gradually declines and stabilizes at a consistent, diminished power level.

Up to 10 seconds after starting the induction motor, the effects of VIF coupling are measured by different parameter values, which have been collected and power calculated from Eq. 5 and summarized in Table 3.

$$P = VI \times PF \tag{5}$$

where the V is equal to Voltage, I is equal to Current in Ampere, and PF, is the power factor, respectively. The power is calculated in watts.

Table 3
The induction motor power calculating parameter values of with and without VIF

Time	With VIF	Without VIF	Power Saving	Overall Saving
Second	Power Consumption	Power Consumption	Watt	In %
1st	551.78	501.63	-50.15	
2nd	552.53	493.75	-58.78	
3rd	493.72	472.12	-21.6	
4th	513.42	529.94	16.52	
5th	489.335	529.70	40.365	5.09
6th	477.4	540.73	63.33	
7th	477.2	528.76	51.56	
8th	465.46	528.76	63.3	
9th	477.4	551.77	74.37	
10th	477.4	551.76	74.36	

4.2 Simulation Vs Prototype Parameter Considerations

In the second case study, a comparative study was done for the simulated result and the consumed power by the prototype. In the prototype case, the short-term variance computation entailed acquiring and archival data by deploying camera recording mechanisms over a brief temporal interval spanning 15 to 30 seconds. Subsequently, the archived data points underwent manual documentation. The system remained uninterrupted for an extended temporal span of approximately thirty seconds, after which the cumulative power consumption was subsequently derived and quantified.

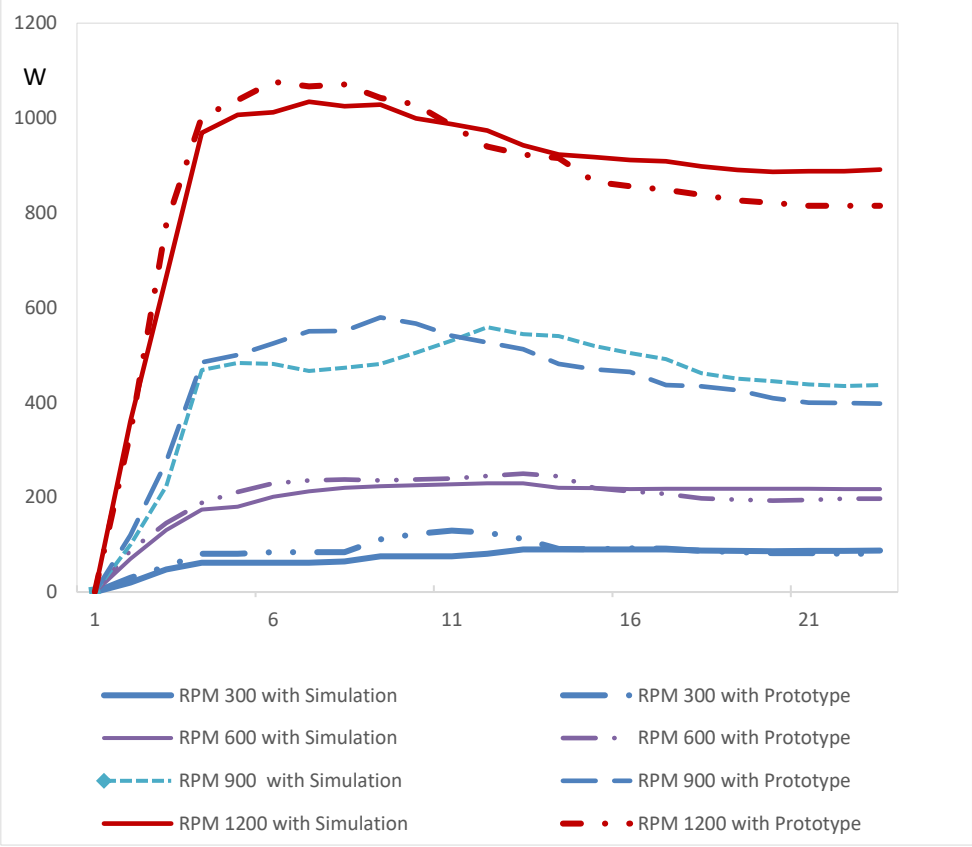

Fig. 5. Comparison between the power consumption with simulation and prototype

Ultimately, Figure 5 has been employed to scrutinize the consumption patterns associated with different velocities, and the overarching observation reveals a notable concurrence between the curve generated by the simulation and the measurements obtained from the physical prototype. When considering variations in speed, it becomes evident that power consumption remains at a lower level during operation under lower-speed conditions, escalating proportionally with speed increments. The association between speed and power is visually depicted in Figure 6, demonstrating an almost linear relationship, albeit with non-uniform incremental values.

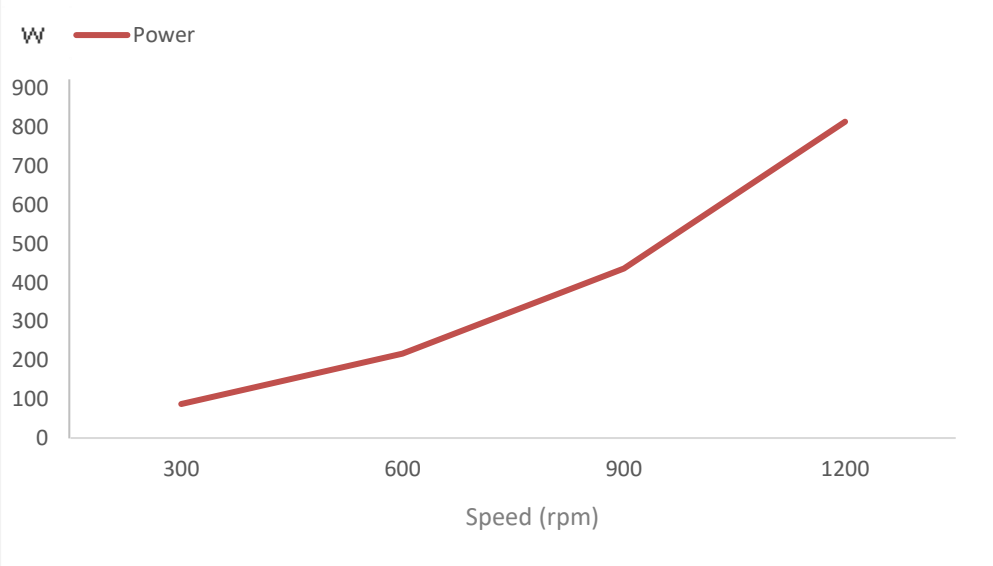

Fig. 6. Comparison of the power consumption with different speed

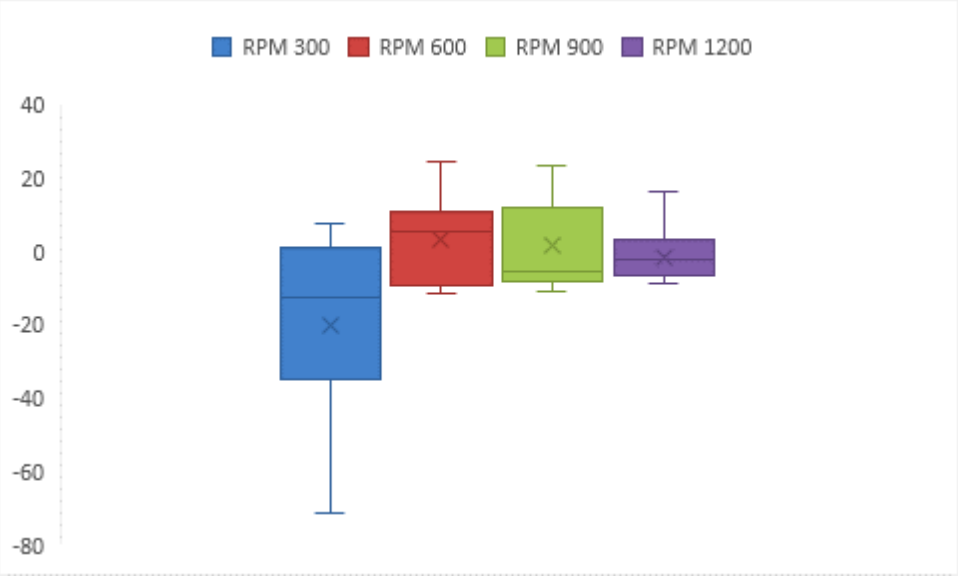

Fig. 7. Average error for the power consumption with different speeds with the simulation

Further, errors were assessed across various speed conditions by comparing the simulated values with the actual data. The presentation of these deviations according to speed is illustrated in Figure 7, revealing that, on average, the discrepancies were not significantly high; however, certain individual values exhibited notable deviations from their corresponding simulated counterparts.

Additionally, by deriving the standard error from the standard deviation values, an overall standard error of merely 3.1 was computed based on the consideration of nearly 100 samples. Consequently, it is inferred that the differences between the simulation and prototype values are relatively minor, and therefore, the simulated values can be confidently employed for future calculations.

Conclusions

The experimental data of the prototype model has been carefully investigated in this research. The dynamic performance of a motor uses a detailed model based on simulation and a prototype to complement the model. In addition to that, the induction motor has been demonstrated both with and without the VIF. Compared to other energy storage methods, VIF significantly requires five percent of reduced power from this system's intake. If a more complicated and comprehensive management strategy is considered, the flywheel's VIF incorporation will result in higher effectiveness. It may be possible to implement trade-offs in the quantity of iron and copper losses designed into the system To optimize the storage system's performance. It can be asserted that the comparison between simulation and practical application yields nearly indistinguishable outcomes, thereby indicating the potential utility of this simulation in optimizing the system, should any modifications be contemplated.

References

[1] M. Farhadi and O. Mohammed, "Energy Storage Technologies for High-Power Applications," IEEE Transactions on Industry Applications 52, no. 3 (2015): 1953-1961. https://doi.org/10.1109/TIA.2015.2511096

[2] M.L. Lazarewicz and A. Rojas, "Grid Frequency Regulation by Recycling Electrical Energy in Flywheels," *IEEE Power Engineering Society General Meeting 2004*, (Denver, Colorado, USA, June 6-10, 2004): 2038-2042. https://doi.org/10.1109/PES.2004.1373235

[3] J.A. Kirk, "Flywheel Energy Storage—I: Basic Concepts," International Journal of Mechanical Sciences 19, no. 4 (1977): 223-231. https://doi.org/10.1016/0020-7403(77)90064-9

[4] M.A. Md Ali, W.N. Azrina, N. Idayu, Z. Abdullah, M.S. Abdul Aziz, S. Subramoniam, N.F.B. Wakhi Anuar and M.H. Abu Bakar, "Fill Time Optimization Analysis in Flow Simulation of Injection Molding Using Response Surface Method," Malaysian Journal on Composites Science and Manufacturing 4, no. 1 (2021): 28-39. https://doi.org/10.37934/mjcsm.4.1.2839

[5] S.M. Salam and M.M. Rashid, "A New Approach to Analysis and Simulation of Flywheel Energy Storage System" In *8th International Conference on Mechatronics Engineering (ICOM 2022)*, Online Conference, Kuala Lumpur, Malaysia, August 9-10, 2022. https://doi.org/10.1049/icp.2022.2271

[6] L. Alhrshy, C. Jauch and P. Kloft, "Development of a Flexible Lightweight Hydraulic-Pneumatic Flywheel System for Wind Turbine Rotors," Fluids 5, no. 4 (2020): 162. https://doi.org/10.3390/fluids5040162

[7] M.P. Figliotti and M.W. Gomes, "A Variable-Inertia Flywheel Model for Regenerative Braking on a Bicycle," *Dynamic Systems and Control Conference* 46193, (Texas, USA: American Society of Mechanical Engineers, October 22-24, 2014): V002T21A004. https://doi.org/10.1115/DSCC2014-6276

[8] J. Van de Ven, "Fluidic Variable Inertia Flywheel,"In *7th International Energy Conversion Engineering Conference*, Denver, Colorado, USA, August 2-5, 2009. https://doi.org/10.2514/6.2009-4501

[9] W.H. Wan Mahmood and U.A.A. Azlan, "QFD Approach in Determining the Best Practices for Green Supply Chain Management in Composite Technology Manufacturing Industries," Malaysian Journal on Composites Science and Manufacturing 1, no. 1 (2020): 45-56. https://doi.org/10.37934/mjcsm.1.1.4556

[10] J. Braid, "Conceptual Design of a Liquid-Based Variable Inertia Flywheel for Microgrid Applications," *2014 IEEE International Energy Conference (ENERGYCON)*, (Dubrovnik, Croatia, May 13-16, 2014): 1291–1296. https://doi.org/10.1109/ENERGYCON.2014.6850589
[11] L.G. Yuan, F.M. Zeng and G.X. Xing, "Research on the Design and Control Strategy of Variable Inertia Flywheel in Diesel Generator Unit Under Pulsed Load," *2010 International Conference on Computing, Control and Industrial Engineering* 1, (Wuhan, China, June 5-6, 2010): 187-189. https://doi.org/10.1109/CCIE.2010.55
[12] E. Bao, H.Y. Hu and D.Y. Liu, "The Theory and Synthesis of High Effect Flywheel with Variable Equivalent Mass Moment of Inertia," Advanced Materials Research 199 (2011): 225–31. https://doi.org/10.4028/www.scientific.net/amr.199-200.225
[13] T. Matsuoka, "Vibration Suppression Device Having Variable Inertia Mass by MR-fluid," *International Design Engineering Technical Conferences and Computers and Information in Engineering Conference* 54785, (Washington DC, USA, August 28-31, 2011): 1181-1185. https://doi.org/10.1115/DETC2011-47020
[14] D. Ullman and H. Velkoff, "An Introduction to the Variable Inertia Flywheel (VIF)," Journal of Applied Mechanics 46, no. 1 (1979): 186–190. https://doi.org/10.1115/1.3424494
[15] A.C. Mahato, S.K. Ghoshal and A.K. Samantaray, "Influence of Variable Inertia Flywheel and Soft Switching on a Power Hydraulic System," SN Applied Sciences 1, no. 6 (2019): 1-13. https://doi.org/10.1007/s42452-019-0623-0
[16] X. Dong, J. Xi, P. Chen and W. Li, "Magneto-rheological Variable Inertia Flywheel," Smart Materials and Structures 27, no. 11 (2018): 115015. https://doi.org/10.1088/1361-665X/aad42b